

# Resonance model study of strangeness production in $pp$ collisions \*

K. Tsushima<sup>1 †</sup>, A. Sibirtsev<sup>2 ‡</sup>, A. W. Thomas<sup>1 §</sup>

<sup>1</sup>Department of Physics and Mathematical Physics  
and Institute for Theoretical Physics

University of Adelaide, SA 5005, Australia

<sup>2</sup>Institut für Theoretische Physik, Universität Giessen  
D-35392 Giessen, Germany

## Abstract

Results for the energy dependence of the elementary kaon production cross sections in proton-proton collisions are reported. Calculations are performed within an extended version of the resonance model which was used for the previous studies of elementary kaon production in pion-nucleon and pion- $\Delta$  collisions. Although the model treatment is within the *empirical* tree level (observed widths for the resonances are used), it is fully relativistic, and includes all relevant baryon resonances up to 2 GeV. One of the purposes of this study is to provide the results for the simulation codes of subthreshold kaon production in heavy ion collisions. This is the first, consistent study of the elementary kaon production reactions including both  $\pi B$  and  $BB$  ( $B = N, \Delta$ ) collisions on the same footing. Comparisons are made between the calculated results and the existing semi-empirical parametrizations which are widely used for the simulation codes, as well as the experimental data.

*PACS:* 24.10.Jv; 25.40.-h; 25.60.Dz; 25.70.-z; 25.70.Ef; 25.75.Dw

*Keywords:* Kaon production; Elementary cross sections; Heavy ion collisions; Baryon resonances; One boson exchange

Strangeness production in heavy ion collisions is presently an issue of intense study. The enhancement of strangeness production in heavy ion collisions might indicate evidence for a new form of nuclear matter, such as a quark gluon plasma [1, 2]. Particularly, kaon production in heavy ion collisions is considered a promising method not only of obtaining information about hot, dense nuclear matter, but also of determining the nuclear equation of state [3, 4, 5].

For the study of kaon production in heavy ion collisions, the elementary cross sections in pion-nucleon and baryon-baryon collisions are some of the most basic and important ingredients for the microscopic calculation of the total kaon yield. However, the available experimental data for the baryon-baryon collision channels are very scarce (most exist for  $pp$  collision channels) and thus could not be parameterized in a satisfactory way for practical use. Indeed, there are

---

\*Supported in part by the Australian Research Council and the Forschungszentrum Jülich

<sup>†</sup>ktsushim@physics.adelaide.edu.au

<sup>‡</sup>sibirt@theorie.physik.uni-giessen.de

<sup>§</sup>athomas@physics.adelaide.edu.au

drastic differences between the commonly used, semi-empirical parametrizations for (the energy dependence of) the total kaon production cross sections in baryon-baryon collisions proposed by Randrup and Ko [6], and Schürmann and Zwermann [7]. Thus, one has to parametrize these cross sections by relying on the theoretical investigations, which also describe the pion-baryon collision channels at the same time.

Although simulation results for kaon production in heavy ion collisions suggest that the  $N\Delta$  and  $\Delta\Delta$  collision channels give the dominant contribution for the total kaon yield [8, 9, 10], the present situation regarding the theoretical investigations seems to be unsatisfactory. In the past, the reactions  $pp \rightarrow NYK$  ( $Y = \Lambda, \Sigma$  hyperons) were investigated within a One Boson Exchange Model (OBEM) by Ferrari [11], Yao [12], Wu and Ko [13], Laget [14] and Deloff [15]. These calculations show quite contradictory contributions from the pion and kaon exchange processes, which can be ascribed to the different values of the coupling constants and cut-off parameters applied. Nevertheless, all of these calculations reproduce almost perfectly *the small number of* available experimental data points. This may imply the necessity of the constraints to fix the pion and kaon contributions consistently by investigating some other appropriate reactions.

Recently, Li and Ko [16], and Sibirtsev [17] performed calculations of kaon production in heavy ion collisions and proton-nucleus collisions, respectively by using the elementary kaon production cross sections calculated using the OBEM. They adopted the results of the resonance model [18, 19, 20] for the elementary cross sections  $\pi B \rightarrow YK$  in order to extract the  $B_1 B_2 \rightarrow B_3 YK$  cross sections. There, an isospin average procedure is introduced for the  $\pi B \rightarrow YK$  cross sections, and the exchanged pion and kaon are treated on their mass shells. Furthermore, although the kaon exchange contribution was included in addition to the pion exchange [16, 17], the  $\eta$  and  $\rho$ -meson exchange contributions were not studied. To be consistent with the resonance model,  $\eta$  and  $\rho$ -meson exchanges should be included, since those resonances included in the model are observed to decay to the  $\eta N$  and  $\rho N$  as well as the  $\pi N$  ( $\pi\Delta$ ) channels [21]. Actually, as will be discussed later, the  $\rho$ -meson exchange gives a dominant contribution in the present calculations.

In this article, we present the results for the energy dependence of the total cross sections  $pp \rightarrow NYK$  calculated in the resonance model [18, 19, 20]. For the other reactions,  $B_1 B_2 \rightarrow B_3 YK$  ( $B_1, B_2, B_3 = N, \Delta$ ), an extensive summary of the results of the study will be reported elsewhere [22].

The advantages of the present investigations are as follows. The resonance model [18, 19, 20] has already been applied to the study of the  $\pi B \rightarrow YK$  ( $B = N, \Delta$ ) reactions. Although the model treatment is within the *empirical* tree level (observed widths for the resonances are used), it is fully relativistic, and includes all relevant baryon resonances up to 2 GeV, which are observed to decay to the hyperon and kaon channels. It turned out that the model was successful in explaining the abundance of available experimental data for the  $\pi N \rightarrow YK$  reactions [24]. This means that the richness of the data can provide a sound basis to the model because the parameters in the model are determined so as to reproduce the whole available data optimally. Thus, many of the effective interactions which are necessary to describe the  $B_1 B_2 \rightarrow B_3 YK$  reactions are fixed within our model. Furthermore, we believe the present calculations are the first systematic calculations for both the  $\pi B \rightarrow YK$  and  $B_1 B_2 \rightarrow B_3 YK$  ( $pp \rightarrow NYK$ ) reactions.

The processes relevant for the present calculations are depicted in Fig. 1. Here  $B^*$  stands for the baryon resonances which decay to the kaon-hyperon channels with their masses up to around 2 GeV [21], namely  $N(1650)(\frac{1}{2}^-)$ ,  $N(1710)(\frac{1}{2}^+)$ ,  $N(1720)(\frac{3}{2}^+)$  and  $\Delta(1920)(\frac{3}{2}^+)$ . In our model, kaons are always assumed to arise from these resonances at the same time as the hyperons. Once the effective Lagrangians and form factors for the vertices are fixed, most of

the relevant coupling constants can be calculated by using the experimental branching ratios. More detailed explanations of the model can be found in refs. [18, 19, 20].

Effective Lagrangian densities necessary to evaluate the Feynman diagrams shown in Fig. 1 are given by,

$$\mathcal{L}_{\pi NN} = -ig_{\pi NN}\bar{N}\gamma_5\vec{\tau}N \cdot \vec{\pi}, \quad (1)$$

$$\mathcal{L}_{\pi NN(1650)} = -g_{\pi NN(1650)}\left(\bar{N}(1650)\vec{\tau}N \cdot \vec{\pi} + \bar{N}\vec{\tau}N(1650) \cdot \vec{\pi}\right), \quad (2)$$

$$\mathcal{L}_{\pi NN(1710)} = -ig_{\pi NN(1710)}\left(\bar{N}(1710)\gamma_5\vec{\tau}N \cdot \vec{\pi} + \bar{N}\vec{\tau}\gamma_5N(1710) \cdot \vec{\pi}\right), \quad (3)$$

$$\mathcal{L}_{\pi NN(1720)} = \frac{g_{\pi NN(1720)}}{m_\pi}\left(\bar{N}^\mu(1720)\vec{\tau}N \cdot \partial_\mu\vec{\pi} + \bar{N}\vec{\tau}N^\mu(1720) \cdot \partial_\mu\vec{\pi}\right), \quad (4)$$

$$\mathcal{L}_{\pi N\Delta(1920)} = \frac{g_{\pi N\Delta(1920)}}{m_\pi}\left(\bar{\Delta}^\mu(1920)\vec{\mathcal{I}}N \cdot \partial_\mu\vec{\pi} + \bar{N}\vec{\mathcal{I}}^\dagger\Delta^\mu(1920) \cdot \partial_\mu\vec{\pi}\right), \quad (5)$$

$$\mathcal{L}_{\eta NN} = -ig_{\eta NN}\bar{N}\gamma_5N\eta, \quad (6)$$

$$\mathcal{L}_{\eta NN(1710)} = -ig_{\eta NN(1710)}\left(\bar{N}(1710)\gamma_5N\eta + \bar{N}\gamma_5N(1710)\eta\right), \quad (7)$$

$$\mathcal{L}_{\eta NN(1720)} = \frac{g_{\eta NN(1720)}}{m_\eta}\left(\bar{N}^\mu(1720)N\partial_\mu\eta + \bar{N}N^\mu(1720)\partial_\mu\eta\right), \quad (8)$$

$$\mathcal{L}_{\rho NN} = -g_{\rho NN}\left(\bar{N}\gamma^\mu\vec{\tau}N \cdot \vec{\rho}_\mu + \frac{\kappa}{2m_N}\bar{N}\sigma^{\mu\nu}\vec{\tau}N \cdot \partial_\mu\vec{\rho}_\nu\right), \quad (9)$$

$$\mathcal{L}_{\rho NN(1710)} = -g_{\rho NN(1710)}\left(\bar{N}(1710)\gamma^\mu\vec{\tau}N \cdot \vec{\rho}_\mu + \bar{N}\vec{\tau}\gamma^\mu N(1710) \cdot \vec{\rho}_\mu\right), \quad (10)$$

$$\mathcal{L}_{\rho NN(1720)} = -ig_{\rho NN(1720)}\left(\bar{N}^\mu(1720)\gamma_5\vec{\tau}N \cdot \vec{\rho}_\mu + \bar{N}\vec{\tau}\gamma_5N^\mu(1720) \cdot \vec{\rho}_\mu\right), \quad (11)$$

$$\mathcal{L}_{K\Lambda N(1650)} = -g_{K\Lambda N(1650)}\left(\bar{N}(1650)\Lambda K + \bar{K}\bar{\Lambda}N(1650)\right), \quad (12)$$

$$\mathcal{L}_{K\Sigma N(1710)} = -ig_{K\Lambda N(1710)}\left(\bar{N}(1710)\gamma_5\Lambda K + \bar{K}\bar{\Lambda}\gamma_5N(1710)\right), \quad (13)$$

$$\mathcal{L}_{K\Lambda N(1720)} = \frac{g_{K\Lambda N(1720)}}{m_K}\left(\bar{N}^\mu(1720)\Lambda\partial_\mu K + (\partial_\mu\bar{K})\bar{\Lambda}N^\mu(1720)\right), \quad (14)$$

$$\mathcal{L}_{K\Sigma N(1710)} = -ig_{K\Sigma N(1710)}\left(\bar{N}(1710)\gamma_5\vec{\tau} \cdot \vec{\Sigma}K + \bar{K}\vec{\Sigma} \cdot \vec{\tau}\gamma_5N(1710)\right), \quad (15)$$

$$\mathcal{L}_{K\Sigma N(1720)} = \frac{g_{K\Sigma N(1720)}}{m_K}\left(\bar{N}^\mu(1720)\vec{\tau} \cdot \vec{\Sigma}\partial_\mu K + (\partial_\mu\bar{K})\vec{\Sigma} \cdot \vec{\tau}N^\mu(1720)\right), \quad (16)$$

$$\mathcal{L}_{K\Sigma\Delta(1920)} = \frac{g_{K\Sigma\Delta(1920)}}{m_K}\left(\bar{\Delta}^\mu(1920)\vec{\mathcal{I}} \cdot \vec{\Sigma}\partial_\mu K + (\partial_\mu\bar{K})\vec{\Sigma} \cdot \vec{\mathcal{I}}^\dagger\Delta^\mu(1920)\right). \quad (17)$$

The notation and definitions appearing in the above equations are as follows:  $\vec{\mathcal{I}}$  is the transition operator defined by

$$\vec{\mathcal{I}}_{M\mu} = \sum_{\ell=\pm 1,0} (1\ell\frac{1}{2}\mu|\frac{3}{2}M)\hat{e}_\ell^*, \quad (18)$$

with  $M$  and  $\mu$  being the third components of the isospin states, and  $\vec{\tau}$  the Pauli matrices.  $N, N(1710), N(1720)$  and  $\Delta(1920)$  stand for the fields of the nucleon and baryon resonances. They are expressed by  $\bar{N} = (\bar{p}, \bar{n})$ , similarly for the nucleon resonances, and  $\bar{\Delta}(1920) = (\bar{\Delta}(1920)^{++}, \bar{\Delta}(1920)^+, \bar{\Delta}(1920)^0, \bar{\Delta}(1920)^-)$  in isospin space. The physical representations of the fields are,  $K^T = (K^+, K^0)$ ,  $\bar{K} = (K^-, \bar{K}^0)$ ,  $\pi^\pm = (\pi_1 \mp i\pi_2)/\sqrt{2}$ ,  $\pi^0 = \pi_3$ , similarly for the  $\rho$ -meson fields, and  $\Sigma^\pm = (\Sigma_1 \mp i\Sigma_2)/\sqrt{2}$ ,  $\Sigma^0 = \Sigma_3$ , respectively, where the superscript  $T$  means the transposition operation. The meson fields are defined as annihilating (creating) the physical particle (anti-particle) states. For the propagators  $iS_F(p)$  of the spin 1/2 and  $iG^{\mu\nu}(p)$  of the spin 3/2 resonances we use:

$$iS_F(p) = i\frac{\gamma \cdot p + m}{p^2 - m^2 + im\Gamma^{full}}, \quad (19)$$

$$iG^{\mu\nu}(p) = i \frac{-P^{\mu\nu}(p)}{p^2 - m^2 + im\Gamma^{full}}, \quad (20)$$

with

$$P^{\mu\nu}(p) = -(\gamma \cdot p + m) \left[ g^{\mu\nu} - \frac{1}{3} \gamma^\mu \gamma^\nu - \frac{1}{3m} (\gamma^\mu p^\nu - \gamma^\nu p^\mu) - \frac{2}{3m^2} p^\mu p^\nu \right], \quad (21)$$

where  $m$  and  $\Gamma^{full}$  stand for the mass and full decay width of the corresponding resonances. For the form factors  $F(\vec{q})$  attached to the meson-resonance vertices, we use

$$F(\vec{q}) = \frac{\Lambda^2}{\Lambda^2 + \vec{q}^2}, \quad (22)$$

where  $\vec{q}$  and  $\Lambda$  are the three momentum of the meson and cut-off parameter, respectively. The form factors, coupling constants and cut-off parameters are adopted from refs. [18, 19, 20]<sup>1</sup>. For the cut-off parameters in the  $\eta NB^*$  and  $\rho NB^*$  vertex form factors in  $pp$  (baryon-baryon) collisions which have not appeared in earlier work, we use the same values as those for the  $\pi NB^*$  vertices in order to reduce the number of new parameters. The other coupling constants, cut-off parameters and form factors are, as far as possible, taken from the Bonn nucleon-nucleon potential model [23] (Model I in TABLE B.1). We use a dipole form factor and the tensor coupling constant is given by the ratio  $\kappa = f_{\rho NN}/g_{\rho NN} = 6.1$  for the  $\rho NN$  vertex. In order to show the structure of total amplitude in terms of the meson exchange and resonance intermediate states, we explicitly write down the contributions for the  $pp \rightarrow p\Lambda K^+$  reaction as an example:

$$\begin{aligned} \mathcal{M}(pp \rightarrow p\Lambda K^+) &= \mathcal{M}(\pi, N(1650)) + \mathcal{M}(\pi, N(1710)) + \mathcal{M}(\pi, N(1720)) \\ &+ \mathcal{M}(\eta, N(1710)) + \mathcal{M}(\eta, N(1720)) + \mathcal{M}(\rho, N(1710)) + \mathcal{M}(\rho, N(1720)) \\ &+ \text{exchange}. \end{aligned} \quad (23)$$

On the right hand side of eq. (23), the exchanged mesons and intermediate state resonances are written inside the brackets (c.f. Fig. 1). Since there is no way to fix adequately the relative signs among the amplitudes, we simply neglect all the interference terms (including the exchange terms). For example, the total amplitude for  $pp \rightarrow p\Lambda K^+$  given by eq. (23) contains fourteen different amplitudes including the exchange amplitudes (diagram b) in Fig. 1), which have relative minus signs to the corresponding direct amplitudes (diagram a) in Fig. 1). Thus there arise  $2^6$  different possible relative sign combinations among them. Concerning the interference effects between the direct and exchange amplitudes, we comment as follows. At energy 1 GeV above the threshold, we calculated the absolute ratios between the direct and exchange amplitudes for the  $\rho$ -meson exchange (which gives dominant contribution in our model) in order to make a rough estimate of the interference effects for the  $pp \rightarrow p\Lambda K^+$  reaction. It turned out that the direct (exchange) process gave a dominant contribution when the final proton was scattered in the forward (backward) direction. The absolute ratios of the direct and exchange amplitudes were typically a few percent, when the absolute values of the amplitudes became large and gave dominant contributions to the cross sections. Furthermore, when the final proton stopped, a sum of the absolute values of the direct and the exchange amplitudes amounted to at most about a 10 percent of the forward (backward) scattering case. Although the interference effects between the direct and exchange processes could be important near the threshold, the effects seems to be small around 1 GeV above the threshold, where the new parameters of the

---

<sup>1</sup>The coupling constants for  $g_{K\Sigma N(1710)}^2$  and  $g_{K\Sigma N(1720)}^2$  in the tables of refs. [18, 19] were listed wrongly, although the numerical calculations were performed by using the correct values as given in this article.

Table 1: Coupling constants and cut-off parameters.  $\kappa = f_{\rho NN}/g_{\rho NN} = 6.1$  for the  $\rho NN$  tensor coupling is used. The confidence levels of the resonances listed below are, N(1650)\*\*\*\*, N(1710)\*\*\*, N(1720)\*\*\*\* and  $\Delta(1920)$ \*\*\* [21].

vertex	$g^2/4\pi$	cut-off (MeV)	vertex	$g^2/4\pi$	cut-off (MeV)
$\pi NN$	14.4	1050	$\pi NN(1650)$	$1.12 \times 10^{-1}$	800
$\pi NN(1710)$	$2.05 \times 10^{-1}$	800	$\pi NN(1720)$	$4.13 \times 10^{-3}$	800
$\pi N\Delta(1920)$	$1.13 \times 10^{-1}$	500	$\eta NN$	5.00	2000
$\eta NN(1710)$	2.31	800	$\eta NN(1720)$	$1.03 \times 10^{-1}$	800
$\rho NN$	0.74	920	$\rho NN(1710)$	$3.61 \times 10^{+1}$	800
$\rho NN(1720)$	$1.43 \times 10^{+2}$	800	$K\Lambda N(1650)$	$5.10 \times 10^{-2}$	800
$K\Lambda N(1710)$	3.78	800	$K\Lambda N(1720)$	$3.12 \times 10^{-1}$	800
$K\Sigma N(1710)$	4.66	800	$K\Sigma N(1720)$	$2.99 \times 10^{-1}$	800
$K\Sigma\Delta(1920)$	$3.08 \times 10^{-1}$	500			

model were fitted to the data. The effects of interference terms were studied in refs. [18, 19] for the  $\pi B$  collision channels, and it turned out that their effects to the shape of the differential cross sections were appreciable, but their effects to the total cross sections were small.

For completeness, we give the relations between the  $K^+$  and  $K^0$  production cross sections treated in this article as follows:

$$\sigma(pp \rightarrow p\Lambda K^+) = \sigma(nn \rightarrow n\Lambda K^0), \quad (24)$$

$$\sigma(nn \rightarrow n\Sigma^- K^+) = \sigma(pp \rightarrow p\Sigma^+ K^0), \quad (25)$$

$$\sigma(pp \rightarrow p\Sigma^0 K^+) = \sigma(nn \rightarrow n\Sigma^0 K^0), \quad (26)$$

$$\sigma(pp \rightarrow n\Sigma^+ K^+) = \sigma(nn \rightarrow n\Sigma^- K^0). \quad (27)$$

Here it should be mentioned that the  $\rho$  meson exchange turned out to give a dominant contribution in the present calculations, as mentioned before. In order to reproduce all the available data in a satisfactory manner, the coupling constant  $g_{\rho NN}$  and cut-off parameter  $\Lambda_\rho$  were varied. The dependence on these quantities is discussed below.

In Fig. 2, the dependence on the coupling constant  $g_{\rho NN}$  of the total cross section  $pp \rightarrow p\Lambda K^+$  is shown. Here,  $s^{1/2}$  is the invariant collision energy in the proton-proton center-of-momentum system, and  $s_0^{1/2} = m_N + m_Y + m_K$  is the threshold energy, with  $m_N$ ,  $m_Y$  and  $m_K$  being the masses of the nucleon, hyperon and kaon, respectively. After fixing the cut-off parameter  $\Lambda_\rho$  to a specific value, the dependence on the coupling constant is small.

Sensitivity of the total cross section  $pp \rightarrow p\Lambda K^+$  to the cut-off parameter values  $\Lambda_\rho$  are shown in Fig. 3 with the experimental data [24]. The dependence on the cut-off parameter  $\Lambda_\rho$  is rather large in the present calculation, after fixing the coupling constant  $g_{\rho NN}$  (and  $\kappa=6.1$  for the tensor coupling constant) to adequate, *non-small* values.

After all, the best values obtained to reproduce the experimental data are,  $g_{\rho NN}^2/4\pi = 0.74$  and  $\Lambda_\rho = 920$  MeV. We summarize in Table 1 all the relevant coupling constants and cut-off parameters determined and used for the calculations in our model.

In Fig. 4 we show the calculated energy dependence of the total cross sections  $pp \rightarrow p\Sigma^+ K^0$ ,  $pp \rightarrow p\Sigma^0 K^+$  and  $pp \rightarrow n\Sigma^+ K^+$  in comparison with the experimental data [24]. The variations

of the experimental data are rather large, but our model can simultaneously reproduce these data well. Remember that we do not have so much freedom in the number of parameters to be varied.

Now we compare our results with some of the existing semi-empirical parametrizations for the energy dependence of the total cross section  $pp \rightarrow p\Lambda K^+$ . In Fig. 5, the dashed-dotted, the dotted, the dashed and the solid lines stand for the parametrizations of Randrup and Ko [6], Schürmann and Zwermann [7], OBEM results of Sibirtsev [17], and our results, respectively. They illustrate quite different energy dependence and strongly disagree when the collision energy,  $s^{1/2}$ , is close to the reaction threshold, except that the results of Sibirtsev [17] and the present calculations show similar behaviour. We should mention here that Li and Ko [16] obtained similar results to ours by applying kaon and pion exchanges. There, the pion and kaon exchanges give almost the same contributions for the  $pp \rightarrow p\Lambda K^+$  total cross sections, while the pion exchange alone gives almost sufficient contribution for the  $pp \rightarrow p\Sigma K$  cross sections. In our model, however, kaon exchange does not enter the calculation, since kaons are assumed to appear together with hyperons through the intermediate state baryon resonances. Furthermore, the exchanged mesons in our model,  $\pi$ ,  $\eta$  and  $\rho$  mesons are adopted based on the observed decay channels of these baryon resonances. However, the contribution of the  $\eta$  meson exchange in our model is small.

We believe the strangeness production in  $pp$  collisions, which is currently being performed at COSY-Jülich [25], will provide important data to improve our understanding of the elementary kaon production mechanism.

In summary, we have presented new calculations for the energy dependence of the total kaon production cross sections in proton-proton collisions using the resonance model. The results reported in this article are part of the systematic studies for both the pion-baryon and baryon-baryon collision channels. The investigations for *free space* will be complete in the near future [22]. The next task to be done is to incorporate the effects of the medium on these elementary kaon production cross sections, which can be implemented in a unified manner based on the same model. Then, we hope that those in-medium modified cross sections can be applied to more realistic investigations of kaon production in heavy ion and proton-nucleus collisions.

### Acknowledgement:

A. S. would like to thank W. Cassing, C.M. Ko and U. Mosel for productive discussions. This work was supported in part by the Australian Research Council and the Forschungszentrum Jülich.

## References

- [1] J. Rafelski and B. Müller, Phys. Rev. Lett. 48 (1982) 1066.
- [2] S. Nagamiya, Nucl. Phys. A544 (1992) 5.
- [3] J. Aichelin and C. M. Ko, Phys. Rev. Lett. 55 (1985) 2661.
- [4] U. Mosel, Annu. Rev. Part. Sci. 41 (1991) 29.
- [5] G. Q. Li and C.M. Ko, Phys. Lett. B349 (1995) 405.
- [6] J. Randrup and C.M. Ko., Nucl. Phys. A343 (1980) 519; Nucl. Phys. A411 (1983) 537.
- [7] B. Schürmann and W. Zwermann, Phys. Lett. B183 (1987) 31.

- [8] A.Lang, W. Cassing, U. Mosel and K. Weber, Nucl. Phys. A541 (1992) 507.
- [9] X. S. Fang, C. M. Ko, G. Q. Li, Y. M. Zheng, Nucl. Phys. A575 (1994) 766.
- [10] C. Hartnack, J. Jaenicke, L. Sehn, H. Stöcker, J. Aichelin, Nucl. Phys. A 580 (1994) 643.
- [11] E. Ferrari, Nuovo Cim. 15 (1960) 652.
- [12] T. Yao, Phys. Rev. 125 (1962) 1048.
- [13] J.Q. Wu and C.M. Ko, Nucl. Phys. A499 (1989) 810.
- [14] J.M. Laget, Phys. Lett. B259 (1991) 24.
- [15] A. Deloff, Nucl. Phys. A505 (1989) 583.
- [16] G.Q. Li and C.M. Ko, Nucl. Phys. A594 (1995) 439.
- [17] A. Sibirtsev, Phys. Lett. B359 (1995) 29; A. Sibirtsev, submitted to Z. Phys. A (1995).
- [18] K. Tsushima, S.W. Huang and A. Faessler, Phys. Lett. B337 (1994) 245.
- [19] K. Tsushima, S.W. Huang and A. Faessler, J. Phys. G21 (1995) 33.
- [20] K. Tsushima, S.W. Huang and A. Faessler, to appear in Australian Journal of Physics, 50, nucl-th/9602005, ADP-96-4/T209.
- [21] Particle Data Group, Phys. Rev. D 45 (1992); *ibid*, D 50 (1994) 1173.
- [22] K. Tsushima, A. Sibirtsev, A. W. Thomas, in preparation.
- [23] R. Machleidt, Adv. in Nucl. Phys. 19 (1989) 189.
- [24] Landolt-Börnstein, New Series, ed. H. Schopper, I/12 (1988).
- [25] U.Bechstedt et al., Annu. Rep. KFA-Jülich (1995) 5.

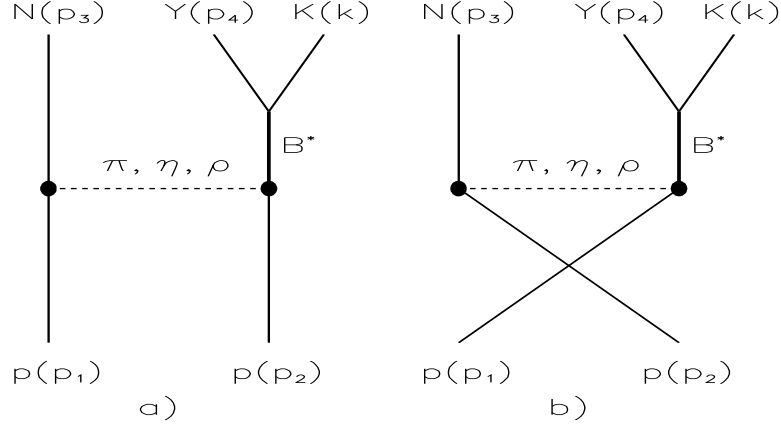


Figure 1: Processes contribute to kaon production in  $pp$  collisions. In figure,  $B^*$  stands for the resonances which are observed to decay to kaon (K) and hyperons ( $Y = \Lambda, \Sigma$ ) up to their masses around 2 GeV. They are,  $N(1650)(\frac{1}{2}^-)$ ,  $N(1710)(\frac{1}{2}^+)$ ,  $N(1720)(\frac{3}{2}^+)$  and  $\Delta(1920)(\frac{3}{2}^+)$ . The exchanged mesons  $\pi$ ,  $\eta$  and  $\rho$  are experimentally observed in these resonance decay channels.



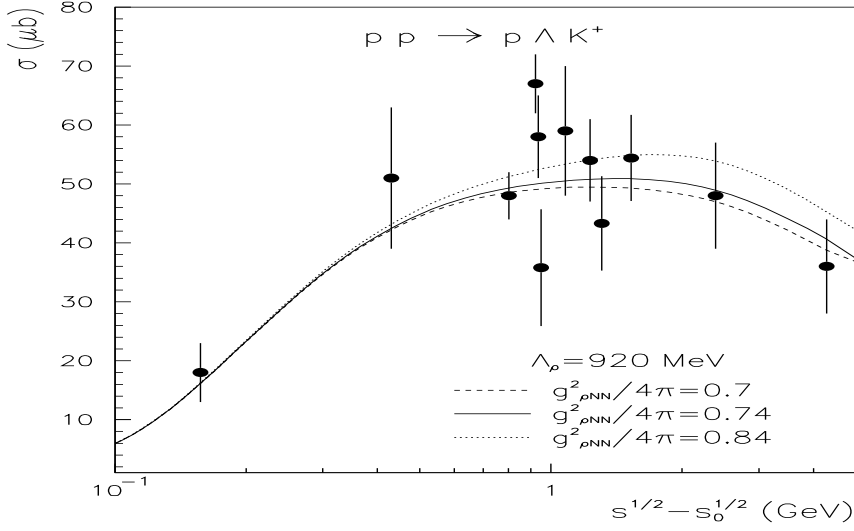


Figure 2: Dependence on the coupling constant  $g_{\rho NN}$  of the total cross section  $pp \rightarrow p\Lambda K^+$ . The dotted, the solid, and the dashed lines show the results obtained with the coupling constant values  $g_{\rho NN}^2/4\pi=0.84$ ,  $g_{\rho NN}^2/4\pi=0.74$ , and  $g_{\rho NN}^2/4\pi=0.70$  with the cut-off parameter  $\Lambda_\rho = 920$  MeV, respectively. The dots show experimental data [24] with error bars.

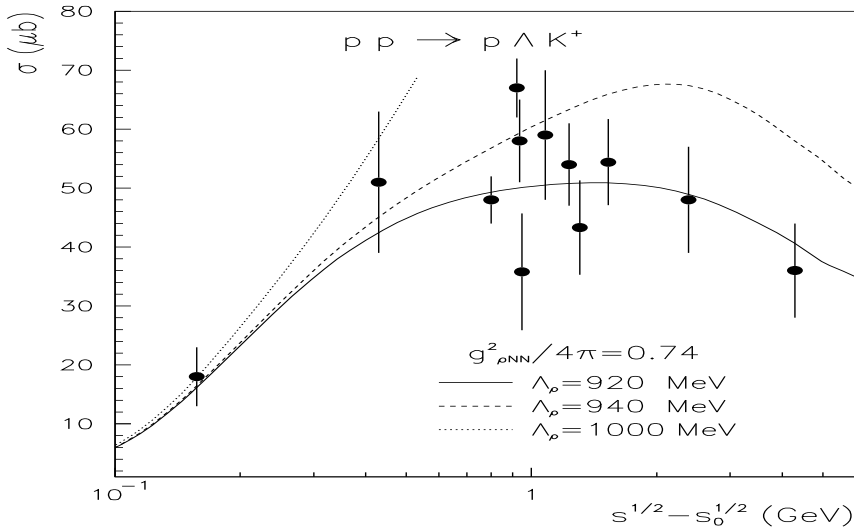


Figure 3: Sensitivities of the total cross section  $pp \rightarrow p\Lambda K^+$  to the cut-off parameters  $\Lambda_\rho$  with experimental data [24]. The dotted, the dashed and the solid lines are the results obtained with the cut-off parameter values  $\Lambda_\rho = 1000$  MeV,  $\Lambda_\rho = 940$  MeV and  $\Lambda_\rho = 920$  MeV, respectively. The coupling constant value is fixed to  $g_{\rho NN}^2/4\pi = 0.74$ .

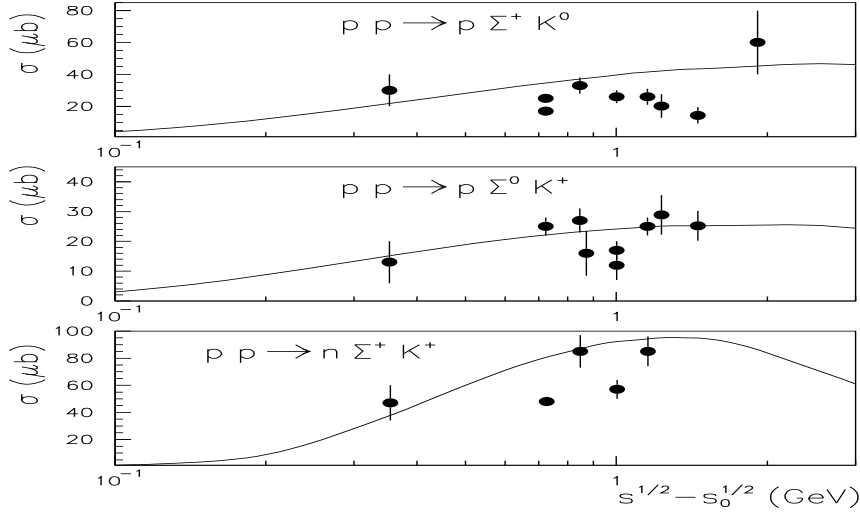


Figure 4: Energy dependence of the total cross sections for the  $pp \rightarrow p\Sigma^+K^0$ ,  $pp \rightarrow p\Sigma^0K^+$  and  $pp \rightarrow n\Sigma^+K^+$  reactions. The dots stand for the experimental data [24] with error bars. The solid lines show our results.

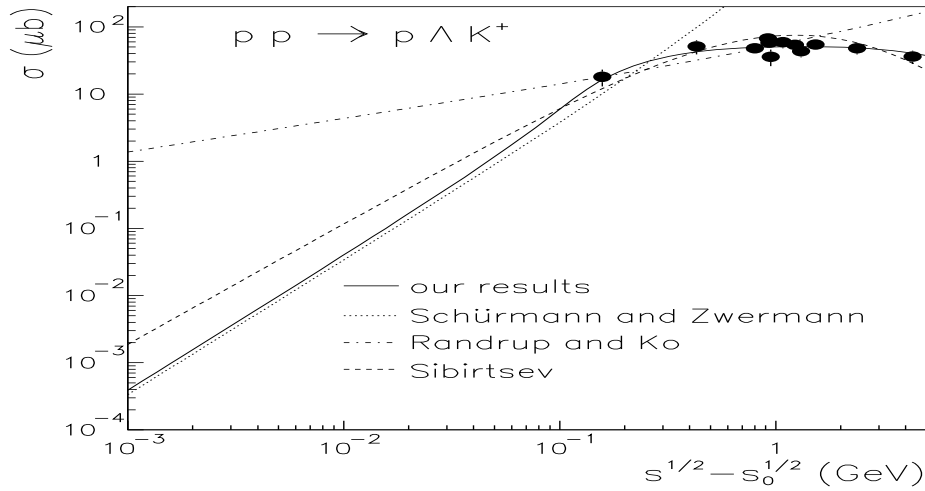


Figure 5: Comparisons between the existing semi-empirical parametrizations and our results for the energy dependence of the total cross section  $pp \rightarrow p\Lambda K^+$ . The dotted, the dashed-dotted, the dashed, and the solid lines stand for the parametrizations of Schürmann and Zwermann [7], Randrup and Ko [6], OBEM results of Sibirtsev [17], and our results, respectively.